

Human-Guided Planning for Complex Manipulation Tasks Using the Screw Geometry of Motion

Dasharadhan Mahalingam

Department of Mechanical Engineering

Stony Brook University

Stony Brook, NY 11794

Email: dasharadhan.mahalingam@stonybrook.edu

Nilanjan Chakraborty

Department of Mechanical Engineering

Stony Brook University

Stony Brook, NY 11794

Email: nilanjan.chakraborty@stonybrook.edu

Abstract—In this paper, we present a novel method for motion planning for performing complex manipulation tasks by using human demonstration and exploiting the screw geometry of motion. We consider complex manipulation tasks where there are constraints on the motion of the end effector of the robot. Examples of such tasks include opening a door, opening a drawer, transferring granular material from one container to another with a spoon, and loading dishes to a dishwasher. Our approach consists of two steps: First, using the fact that a motion in the task space of the robot can be approximated by using a sequence of constant screw motions, we segment a human demonstration into a sequence of constant screw motions. Second, we use the segmented screws to generate motion plans via screw-linear interpolation for other instances of the same task. The use of screw segmentation allows us to capture the invariants of the demonstrations in a coordinate-free fashion, thus allowing us to plan for different task instances from just one example. We present extensive experimental results on a variety of manipulation scenarios showing that our method can be used across a wide range of manipulation tasks.

I. INTRODUCTION

The use of robot manipulators in service industry, domestic environments, as well as in assistive robotics to help people who have lost the use of hands, depends on the ability of the robots to perform *complex manipulation tasks*. Complex manipulation tasks, as opposed to simple reaching or pick-and-place tasks, are characterized by the presence of constraints on the motion of the end effector of the robot. Figure 1 shows some typical complex manipulation tasks, where the constraints can arise from the mechanical structure of the objects (top row) or from the nature of the task itself (bottom row). Operating articulated objects (like opening/closing doors, windows, drawers, and bottle caps) imposes constraints on the motion of the robot end effector depending on the type of the joint (like revolute, prismatic, and helical).

Furthermore, tasks like scooping and pouring, loading a dish into a dishwasher rack, requires constraints on the motion of the end effector. These constraints essentially characterize the task (please see the results section for a more detailed discussion) and the constraints may change during the motion. For example, in the scooping and pouring task in Figure 1, the spoon should not rotate while transferring, it should not translate while pouring and during scooping there is a different constraint on the motion which is hard to describe.



Fig. 1: TYPICAL COMPLEX MANIPULATION TASKS: (Clockwise from top left) Manipulation of object constrained by a revolute joint; Manipulation of object constrained by a prismatic joint; Arranging dishes in a dish rack; Scooping and pouring

Typically, for the robot to perform the task, a robotics expert needs to come up with a mathematical representation of these constraints (which may not always be easy, think about the scooping task) and they need to be pre-programmed. However, many modern light weight cobots like Baxter (Rethink Robotics), Panda (Franka Emika) and UR-3, UR-5, UR-10 (Universal Robots) are designed with easily accessible tools to allow a non-expert in robotics to give a kinesthetic demonstration, i.e., hold the hand of the robot and show how to do a task. Any constraint that characterizes the task is *embedded in these demonstrations*. Therefore, in principle, it is possible to utilize these constraints (even from a single example) for motion planning for a different instance of the task. Note that an instance of a task, or task instance for short, is defined by the poses of task-related objects. Different task instances correspond to different poses of the task-related objects for the same task. *The goal of this paper is to develop a method that can utilize the embedded task constraints in a single kinesthetic demonstration of a task from a human to plan motions for a different instance of the same task.*

The end-effector motion of a robot is a curve in the group of rigid body motions, i.e., $SE(3)$. Our approach is based on exploiting the following characteristic of rigid body motion in $SE(3)$ which is implied by Chasles theorem: *Any curve in*

$SE(3)$, which represents a rigid body motion, can be approximated arbitrarily closely by a sequence of constant screw motions (or one-parameter subgroups of $SE(3)$). Note that when the end-effector motion is constrained by a mechanical joint, its motion is a single constant screw motion, i.e., the motion is constrained to lie in a one-parameter subgroup of $SE(3)$ [21].

Based on the above observation, we present a novel two-step solution approach: (a) Given a kinesthetic demonstration of a task, we segment the motion of the end effector in the task space into a sequence of constant screws. (b) For the new task instance, using the segmented screws, we compute a motion plan based on Screw linear interpolation (ScLERP) which automatically ensures that the constant screw constraints embedded in the demonstrated motion are satisfied. The sequence of constant screws represent the task constraints in a coordinate invariant manner, i.e., it does not depend on the location of the reference frame on the end-effector. By extracting the task constraints which are enforced either due to the presence of joints or due to the inherent nature of the task, we are able to generalize a single demonstration to different task instances. This two-step motion planning method is the *key contribution* of this paper. We also provide extensive experimental results that validates the ability of our approach to generalize from a single example. The key novelty of our method is the combination of data with classical ideas in screw theory that exploits the natural kinematic structure of motion. We show that exploiting the structure of motion can lead to data-efficient approaches for planning using human demonstration as a guide.

II. RELATED WORK

Manipulation of objects in general enforces constraints on the end-effector of the robot. Irrespective of whether these constraints are enforced due to the presence of physical joints (Eg. prismatic, revolute joints), or are enforced as a characteristic of the task even though such physical joints are not present (Eg. scooping contents from a bowl), constrained manipulation is essential to enable robots to interact with its environment and perform tasks successfully. Learning from Demonstration (LfD) [2] is a framework that utilizes demonstrations of tasks acquired either through observation or tele-operation or kinesthetically to make robots perform tasks autonomously by learning these constraints from demonstrations. LfD approaches aim to extract these task constraints either implicitly or explicitly, which are then used to compute the motion plan required to execute the a new instance of the same task.

Dynamic Movement Primitives (DMP) [9], [7], [18], [22] allow learning of control policies from demonstrations. While DMP based approaches can work with a single demonstration, they are generally not used for manipulation of physically constrained objects. DMPs require a new goal configuration as an input. However, the computation of the new goal configuration for articulated motion can only be done if the physical constraints are known explicitly. Machine Learning based approaches to LfD utilizing Gaussian Mixture Models (GMM)

[4] or Hidden Markov Models (HMM) [3], [5] to encode the task information require multiple demonstrations. Trajectory segmentation based approaches that decompose complex movements as a sequence of primitive motions such as [14], [12] either require a predefined library of primitive motions or multiple demonstrations of a task to extract the sequence of primitive motions from the demonstrations. Approaches to manipulate articulated objects such as [10], [24], [25], [1], [20] determine the joint constraints explicitly from provided demonstrations or observations. This would allow to compute the motion plan required for a new task instance by applying this geometric constraint to the motion of the end-effector. The LfD approaches mentioned above can be applied to either one of the following task categories: 1) Manipulation of objects that are not constrained by physical joints 2) Manipulation of objects constrained by physical joints. While the above approaches have been developed specifically for one of the above categories, they might fail or not generalize well on the tasks belonging to the other category. Our approach aims to utilize a unified approach that works well for tasks belonging to both categories. A task space based approach to use provided demonstrations for performing tasks by interpolating between guiding poses using screw linear interpolation has been studied previously in [11]. However, this method has some limitations when considering manipulation of constrained objects. This work extends on [11] for manipulating constrained objects and to also provide a better heuristic for selecting guiding poses from a demonstration. We segment the motion as a sequence of constant screws and enforce this sequence of constant screw constraints on the end-effector. Motion Planning with screw motion constraints on the end-effector has been explored in [21]. By extracting the sequence of constant screw motion constraints that are enforced on the end-effector for everyday tasks from provided demonstrations, the required motion for a new task instance is determined using [21] which ensures that the constant screw constraints are satisfied.

III. MATHEMATICAL PRELIMINARIES

In this section, we present the background knowledge on rigid body motion and screw geometry of rigid body motion required for this work.

Quaternions and Rotations: The quaternions are the set of hypercomplex numbers, \mathbb{H} . A quaternion $\mathbf{Q} \in \mathbb{H}$ can be represented as a 4-tuple $\mathbf{Q} = (q_0, \mathbf{q}_r) = (q_0, q_1, q_2, q_3)$, $q_0 \in \mathbb{R}$ is the real scalar part, $\mathbf{q}_r = (q_1, q_2, q_3) \in \mathbb{R}^3$ corresponds to the imaginary part. The conjugate, norm, and inverse of a quaternion \mathbf{Q} is given by $\mathbf{Q}^* = (q_0, -\mathbf{q}_r)$, $\|\mathbf{Q}\| = \sqrt{\mathbf{Q}\mathbf{Q}^*} = \sqrt{\mathbf{Q}^*\mathbf{Q}}$, and $\mathbf{Q}^{-1} = \mathbf{Q}^*/\|\mathbf{Q}\|^2$, respectively. Addition and multiplication of two quaternions $\mathbf{P} = (p_0, \mathbf{p}_r)$ and $\mathbf{Q} = (q_0, \mathbf{q}_r)$ are performed as $\mathbf{P} + \mathbf{Q} = (p_0 + q_0, \mathbf{p}_r + \mathbf{q}_r)$ and $\mathbf{PQ} = (p_0q_0 - \mathbf{p}_r \cdot \mathbf{q}_r, p_0\mathbf{q}_r + q_0\mathbf{p}_r + \mathbf{p}_r \times \mathbf{q}_r)$. The quaternion \mathbf{Q} is a *unit quaternion* if $\|\mathbf{Q}\| = 1$, and consequently, $\mathbf{Q}^{-1} = \mathbf{Q}^*$. Unit quaternions are used to represent the set of all rigid body rotations, $SO(3)$, the Special Orthogonal group of dimension 3. Mathematically, $SO(3) = \{\mathbf{R} \in \mathbb{R}^{3 \times 3} \mid \mathbf{R}^T \mathbf{R} = \mathbf{R} \mathbf{R}^T = \mathbf{I}_3, |\mathbf{R}| = 1\}$, where \mathbf{I}_3 is a

3×3 identity matrix and $|\cdot|$ is the determinant operator. The unit quaternion corresponding to a rotation is $\mathbf{Q}_R = (\cos \frac{\theta}{2}, \omega \sin \frac{\theta}{2})$, where $\theta \in [0, \pi]$ is the angle of rotation about a unit axis $\omega \in \mathbb{R}^3$.

Dual Quaternions and Rigid Displacements: In general, dual numbers are defined as $d = a + \epsilon b$ where a and b are elements of an algebraic field, and ϵ is a *dual unit* with $\epsilon^2 = 0, \epsilon \neq 0$. Similarly, a dual quaternion \mathbf{D} is defined as $\mathbf{D} = \mathbf{P} + \epsilon \mathbf{Q}$ where $\mathbf{P}, \mathbf{Q} \in \mathbb{H}$. The conjugate, norm, and inverse of the dual quaternion \mathbf{D} is represented as $\mathbf{D}^* = \mathbf{P}^* + \epsilon \mathbf{Q}^*$, $\|\mathbf{D}\| = \sqrt{\mathbf{D}\mathbf{D}^*} = \sqrt{\mathbf{P}\mathbf{P}^* + \epsilon(\mathbf{P}\mathbf{Q}^* + \mathbf{Q}\mathbf{P}^*)}$, and $\mathbf{D}^{-1} = \mathbf{D}^*/\|\mathbf{D}\|^2$, respectively. Another definition for the conjugate of \mathbf{D} is represented as $\mathbf{D}^\dagger = \mathbf{P}^* - \epsilon \mathbf{Q}^*$. Addition and multiplication of two dual quaternions $\mathbf{D}_1 = \mathbf{P}_1 + \epsilon \mathbf{Q}_1$ and $\mathbf{D}_2 = \mathbf{P}_2 + \epsilon \mathbf{Q}_2$ are performed as $\mathbf{D}_1 + \mathbf{D}_2 = (\mathbf{P}_1 + \mathbf{P}_2) + \epsilon(\mathbf{Q}_1 + \mathbf{Q}_2)$ and $\mathbf{D}_1 \mathbf{D}_2 = (\mathbf{P}_1 \mathbf{P}_2) + \epsilon(\mathbf{P}_1 \mathbf{Q}_2 + \mathbf{Q}_1 \mathbf{P}_2)$. The dual quaternion \mathbf{D} is a *unit dual quaternion* if $\|\mathbf{D}\| = 1$, i.e., $\|\mathbf{P}\| = 1$ and $\mathbf{P}\mathbf{Q}^* + \mathbf{Q}\mathbf{P}^* = 0$, and consequently, $\mathbf{D}^{-1} = \mathbf{D}^*$. Unit dual quaternions can be used to represent the group of rigid body displacements, $SE(3) = \mathbb{R}^3 \times SO(3)$, $SE(3) = \{(\mathbf{R}, \mathbf{p}) \mid \mathbf{R} \in SO(3), \mathbf{p} \in \mathbb{R}^3\}$. An element $\mathbf{T} \in SE(3)$, which is a pose of the rigid body, can also be expressed by a 4×4 homogeneous transformation matrix as $\mathbf{T} = [\begin{smallmatrix} \mathbf{R} & \mathbf{p} \\ \mathbf{0} & 1 \end{smallmatrix}]$ where $\mathbf{0}$ is a 1×3 zero vector. A rigid body displacement (or transformation) is represented by a unit dual quaternion $\mathbf{D}_T = \mathbf{Q}_R + \frac{\epsilon}{2} \mathbf{Q}_p \mathbf{Q}_R$ where \mathbf{Q}_R is the unit quaternion corresponding to rotation and $\mathbf{Q}_p = (0, \mathbf{p}) \in \mathbb{H}$ corresponds to the translation. Here, we define \mathbb{D} to represent the set of unit dual quaternions.

Screw Displacement: Chasles-Mozzi theorem states that the general Euclidean displacement/motion of a rigid body from the origin \mathbf{I} to $\mathbf{T} = (\mathbf{R}, \mathbf{p}) \in SE(3)$ can be expressed as a rotation θ about a fixed axis \mathcal{S} , called the *screw axis*, and a translation d along that axis (see Fig. 2). Plücker coordinates can be used to represent the screw axis by ω and \mathbf{m} , where $\omega \in \mathbb{R}^3$ is a unit vector that represents the direction of the screw axis \mathcal{S} , $\mathbf{m} = \mathbf{r} \times \omega$, and $\mathbf{r} \in \mathbb{R}^3$ is an arbitrary point on the axis. Thus, the screw parameters are defined as $\omega, \mathbf{m}, \theta, h$, where $h = \frac{d}{\theta}$ is the pitch of the screw. In general, $h \geq 0$, with $h = \infty$ for pure translation. When h is finite (infinite), $\theta(d)$ is the magnitude of the screw. A *constant screw motion* is a motion where the parameters ω, \mathbf{m} , and h stays constant throughout the motion.

The screw displacements can be expressed by the dual quaternions as $\mathbf{D}_T = \mathbf{Q}_R + \frac{\epsilon}{2} \mathbf{Q}_p \mathbf{Q}_R = (\cos \frac{\Phi}{2}, L \sin \frac{\Phi}{2})$ where $\Phi = \theta + \epsilon d$ is a dual number and $L = \omega + \epsilon \mathbf{m}$ is a dual vector. A power of the dual quaternion \mathbf{D}_T is then defined as $\mathbf{D}_T^\tau = (\cos \frac{\tau\Phi}{2}, L \sin \frac{\tau\Phi}{2})$, $\tau > 0$.

Screw Linear Interpolation (ScLERP): To perform a one degree-of-freedom smooth screw motion (with a constant rotation and translation rate) between two object poses in $SE(3)$, the screw linear interpolation (ScLERP) can be used. The ScLERP provides a *straight line* in $SE(3)$ which is the closest path between two given poses in $SE(3)$. If the poses are represented by unit dual quaternions \mathbf{D}_1 and \mathbf{D}_2 , the path provided by the ScLERP is derived by $\mathbf{D}(\tau) =$

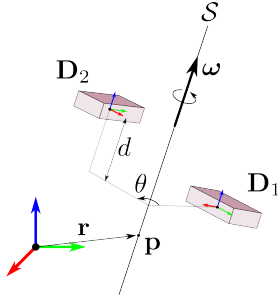


Fig. 2: SCREW DISPLACEMENT FROM POSE \mathbf{D}_1 TO POSE \mathbf{D}_2

$\mathbf{D}_1(\mathbf{D}_1^{-1}\mathbf{D}_2)^\tau$ where $\tau \in [0, 1]$ is a scalar path parameter. As τ increases from 0 to 1, the object moves between two poses along the path $\mathbf{D}(\tau)$ by the rotation $\tau\theta$ and translation τd . Let $\mathbf{D}_{12} = \mathbf{D}_1^{-1}\mathbf{D}_2$. To compute \mathbf{D}_{12}^τ , the screw coordinates $\omega, \mathbf{m}, \theta, d$ are first extracted from $\mathbf{D}_{12} = \mathbf{P} + \epsilon \mathbf{Q} = (p_0, \mathbf{p}_r) + \epsilon(q_0, \mathbf{q}_r) = (\cos \frac{\theta}{2}, \omega \sin \frac{\theta}{2}) + \epsilon \mathbf{Q}$ by $\omega = \mathbf{p}_r/\|\mathbf{p}_r\|$, $\theta = 2 \text{atan2}(\|\mathbf{p}_r\|, p_0)$, $d = \mathbf{p} \cdot \omega$, and $\mathbf{m} = \frac{1}{2}(\mathbf{p} \times \omega + (\mathbf{p} - d\omega) \cot \frac{\theta}{2})$ where \mathbf{p} is derived from $2\mathbf{Q}\mathbf{P}^* = (0, \mathbf{p})$ and $\text{atan2}(\cdot)$ is the two-argument arctangent. Then, $\mathbf{D}_{12}^\tau = (\cos \frac{\tau\theta}{2}, L \sin \frac{\tau\theta}{2})$ is directly derived from $(\cos \frac{\tau\theta}{2}, \sin \frac{\tau\theta}{2}\omega) + \epsilon(-\frac{\tau d}{2} \sin \frac{\tau\theta}{2}, \frac{\tau d}{2} \cos \frac{\tau\theta}{2}\omega + \sin \frac{\tau\theta}{2}\mathbf{m})$. Note that $h = \infty$ corresponds to pure translation.

Distance Metric in $SE(3)$: The heuristic which we follow to determine the distance between two rigid body transformations in space is, to determine the distance in position and orientation separately. Let $\mathbf{D}_1 = \mathbf{Q}_1 + \frac{\epsilon}{2} \mathbf{p}_1 \otimes \mathbf{Q}_1$ and $\mathbf{D}_2 = \mathbf{Q}_2 + \frac{\epsilon}{2} \mathbf{p}_2 \otimes \mathbf{Q}_2$ be two poses in dual quaternion representation.

- The distance in position between two poses is given by the Euclidean norm.

$$d_p(\mathbf{D}_1, \mathbf{D}_2) = \|\mathbf{p}_1 - \mathbf{p}_2\|$$

- The distance in orientation between the two poses as defined in [8] is

$$d_\phi(\mathbf{D}_1, \mathbf{D}_2) = \min(\|\mathbf{Q}_1 - \mathbf{Q}_2\|, \|\mathbf{Q}_1 + \mathbf{Q}_2\|)$$

Neighbourhood of a pose: For any pose that is represented in unit dual quaternions as \mathbf{D} , we define its $(\varepsilon_p, \varepsilon_\phi)$ -neighbourhood as

$$\{\mathbf{D}' \in \mathbb{D} \mid d_p(\mathbf{D}, \mathbf{D}') \leq \varepsilon_p, d_\phi(\mathbf{D}, \mathbf{D}') \leq \varepsilon_\phi\}$$

The parameters ε_p and ε_ϕ define the size of the neighbourhood

IV. PROBLEM STATEMENT

Assume that we have a kinesthetic demonstration of a manipulation task where we have recorded the joint angles of the manipulator during the demonstration (See Figure 3, 11, 13). Using the forward kinematics map, we can obtain the sequence of poses the end effector goes through to accomplish the task. Let $\mathcal{D} := \mathbf{D}_1, \mathbf{D}_2, \dots, \mathbf{D}_n$ be the sequence of task space poses of the end effector and $\mathbf{O}_1, \mathbf{O}_2, \dots, \mathbf{O}_v$ be the poses of the task relevant objects written using a unit dual quaternion representation of $SE(3)$. The sequence of



Fig. 3: DEMONSTRATION FOR MANIPULATION OF ARTICULATED OBJECTS: User provided Kinesthetic demonstration of tasks. Demonstration of manipulating an object constrained by a revolute joint (First and Second images from left; Demonstration 3 of Revolute Joint Experiment); Demonstration of manipulation an object constrained by a prismatic joint (Third and Fourth images from left; Demonstration 3 of Prismatic Joint Experiment)

end effector poses in \mathcal{D} is the task space representation of the demonstrated path. Any task-relevant constraints that characterize the manipulation task are implicitly present in the demonstration. Our goal is to find a motion plan for a new initial and final pose \mathbf{D}'_1 and \mathbf{D}'_n (as well as the new pose of task-relevant objects $\mathbf{O}'_1, \mathbf{O}'_2, \dots, \mathbf{O}'_v$) that utilizes the single demonstration as a guide to perform the desired task instance and incorporates the task-relevant constraints in the new plan. Note that the use of unit dual quaternion representation is not fundamental here (one can as well use the 4×4 transformation matrix representation throughout the whole paper). It is also straightforward and sometimes convenient to go back and forth between the 4×4 transformation matrix representation and the unit dual quaternion representation of $SE(3)$.

To accomplish the above, we use a screw geometry-based representation of the underlying demonstrated motion. In particular, we divide the problem above into two sub-problems.

- 1) **Screw Segmentation Problem:** Given a demonstrated motion in task space and the poses of the task related objects, compute a segmentation of the motion as a sequence of constant screw motions relative to the poses of the task related objects.
- 2) **Motion Generation Problem using Segmented Demonstration:** Given a sequence of constant screw motions that is known to accomplish a given task, for a new task instance of the same task (defined by the initial pose and goal pose of the end effector as well as the poses of the task-relevant objects), compute a motion plan that accomplishes the task instance using the sequence of constant screw motions that was determined from the demonstration.

The rationale for using a screw segmentation of the motion is two-fold. First, from Chasles' theorem it can be inferred that any path in $SE(3)$ can be approximated arbitrarily closely as a sequence of constant screw motions. This is analogous to the fact that any curve in \mathbb{R}^3 can be approximated arbitrarily closely by a sequence of straight line segments. Second, the screw representation is a coordinate-invariant representation (meaning that it does not depend on the choice of the coordinate frame at the end effector of the robot) and also maps the motion to a single parameter subgroup of $SE(3)$, which potentially allows better generalization properties.

V. SCREW SEGMENTATION PROBLEM

In this section, we will discuss the screw segmentation problem and present a solution for the same. Our approach for segmenting the task space motion into constant screws also requires extraction of the screw parameters for each segment. Therefore, for purposes of exposition, we will first discuss the extraction of screws for a motion of the end effector that is generated by a constant screw (e.g., when moving an articulated object like door or drawer whose motion is constrained by a revolute or prismatic joint). Then we will discuss the general case of screw segmentation for a general motion in $SE(3)$. As stated before, we will use a sequence of recorded end-effector poses in dual quaternion representation, $\mathcal{D} = \{\mathbf{D}_1, \mathbf{D}_2, \dots, \mathbf{D}_n\}$.

A. Sequence Generated by a Single Screw

The relative transformation between the initial pose \mathbf{D}_1 and every other pose on the recorded sequence is given by,

$$\mathbf{D}_{1i} = \mathbf{D}_i \otimes \mathbf{D}_1^*, i = 2, 3, \dots, n \quad (1)$$

Where, \mathbf{D}_{1i} is of the form $\mathbf{D}_{1i} = \mathbf{Q}_{1i} + \frac{\epsilon}{2} \mathbf{p}_{1i} \otimes \mathbf{Q}_{1i}$.

Let us consider the sequence $\mathbf{D}_1, \mathbf{D}_2, \dots, \mathbf{D}_n$ to be generated by a single screw with parameters $(\omega, \mathbf{m}, h, \theta)$, with the notations as defined before. If the motion is a general screw motion or pure rotation, then

$$\mathbf{Q}_{1i} = \left(\cos \frac{\theta_{1i}}{2}, \omega \sin \frac{\theta_{1i}}{2} \right) \quad (2)$$

$$\mathbf{p}_{1i} = (\mathbf{I} - e^{\hat{\omega} \theta_{1i}})(\omega \times \mathbf{v}) + \omega \omega^T \mathbf{v} \theta_{1i} \quad (3)$$

where $\mathbf{v} = \mathbf{m} + h\omega$. If the motion is pure translation, then

$$\mathbf{Q}_{1i} = (1, \mathbf{0}) \quad (4)$$

$$\mathbf{p}_{1i} = \omega \theta_{1i} \quad (5)$$

where

$$\omega = \frac{\mathbf{p}_n - \mathbf{p}_1}{\|\mathbf{p}_n - \mathbf{p}_1\|} \quad (6)$$

In both cases, the magnitude of the screw is $\theta = \theta_{1n}$, and $\theta_{1i} = \tau_{1i}\theta$, with $0 \leq \tau_{1i} \leq 1$ and $\tau_{1i} < \tau_{1j}$ for $i < j$. Thus, the entire motion is a one-parameter motion, where the parameter is denoted by τ_{1i} and each end-effector pose corresponds to a different τ_{1i} .

Noiseless Observations: We will first discuss the situation where we assume that there is no noise in the observation.

This is for exposition purposes only, so that the basic idea can be clearly explained. In the subsequent discussion we will look at the noisy case. In the noiseless case, we can take any index i , i.e., any intermediate pose on the recorded path to determine the type of screw motion by computing \mathbf{Q}_{1i} with Equation (2) and (4). Based on the type of screw motion, we use either Equation (2) or (5) to solve for the screw axis ω . Note that the value of θ_{1i} obtained from (2) or (5) will depend on the chosen index i (and it is not part of the screw). The value of ω will be independent of the index chosen and it should be the same for every index $i \geq 2$.

For pure translation, the pitch, $h = \infty$ and $\mathbf{m} = \mathbf{0}$ by definition. For general motion, we can first obtain ω from Equation (2) and \mathbf{v} from Equation (3) using the following expression

$$\mathbf{v} = [(\mathbf{I} - e^{\hat{\omega}\theta_{1i}})\hat{\omega} + \theta_{1i}\omega\omega^T]^{-1} \mathbf{p}_{1i} \quad (7)$$

where the 3×3 matrix $[(\mathbf{I} - e^{\hat{\omega}\theta_{1i}})\hat{\omega} + \theta_{1i}\omega\omega^T]$ is always invertible. Then we get the pitch, h , of the screw using

$$h = \omega^T \mathbf{v} \quad (8)$$

and we get \mathbf{m} by using $\mathbf{m} = \mathbf{v} - h\omega$. If $h = 0$, then the motion is pure rotation.

Noisy Observations: In the presence of noise in observations (which occurs in practical scenarios), the screw parameters extracted from each intermediate pose i may be different. As the screw parameter determination is different for pure translation and general screw/rotational motion, we compute the screw parameters for the motion between the initial pose \mathbf{D}_1 and final pose \mathbf{D}_n by first verifying which of the following hypothesis about the screw motion category are true

- Pure translation ($h = \infty$)
- General screw/pure rotation ($h \neq \infty$)

Ideally, if the sequence $\{\mathbf{D}_1, \mathbf{D}_2, \dots, \mathbf{D}_{n-1}, \mathbf{D}_n\}$ has been generated by a constant screw, then $\forall i \leq n$, there is a θ_{1k} such that, $\mathbf{D}_k = \mathbf{D}_{1k} \otimes \mathbf{D}_n$, where $\mathbf{D}_{1k} = \mathbf{Q}_{1k} + \frac{\epsilon}{2} \mathbf{p}_{1k} \otimes \mathbf{Q}_{1k}$, and has screw parameters $(\omega_{1n}, \mathbf{m}_{1n}, h_{1n}, \theta_{1k})$. But, due to the presence of noise, \mathbf{D}_k does not lie on the ideal screw motion from \mathbf{D}_1 to \mathbf{D}_n . However, using line search on the parameter τ , $0 \leq \tau \leq 1$ we can determine a $\theta_{1k} = \tau\theta_{in}$ which gives us $\mathbf{D}'_k = \mathbf{D}_{1k} \otimes \mathbf{D}_1$ such that \mathbf{D}'_k lies on the screw motion from \mathbf{D}_1 to \mathbf{D}_n and within a neighbourhood $(\epsilon_p, \epsilon_\phi)$ of the pose \mathbf{D}_k . If no such θ_{1k} exists then \mathbf{D}_k does not lie on the screw motion from \mathbf{D}_1 to \mathbf{D}_n . We will be using this to verify if the given sequence \mathcal{D} can be generated from a constant screw and also to check which of the two hypothesis is true.

Algorithm 1 gives the procedure to check if the given motion \mathcal{D} belongs to the category of pure translation ($h = \infty$). Given the motion \mathcal{D} and the parameters $\epsilon_p, \epsilon_\phi$ to define the size of the neighborhood, the algorithm returns true if the motion \mathcal{D} is pure translation and false otherwise. The screw parameters are computed from the initial pose \mathbf{D}_1 and final pose \mathbf{D}_n and then used to determine if each of the intermediate poses \mathbf{D}_i , $2 \leq i \leq n-1$ lie within a neighborhood $(\epsilon_p, \epsilon_\phi)$ of the ideal screw motion from \mathbf{D}_1 to \mathbf{D}_n inside the loop from lines 4 to 8.

Algorithm 1: Check if motion is pure translation

```

1 def checkIfPrismatic( $\mathcal{D}, \epsilon_p, \epsilon_\phi$ ):
2   Determine  $\mathbf{p}_{1n}$  from  $\mathbf{D}_{1n} = \mathbf{D}_n \otimes \mathbf{D}_1^*$ 
3   Compute  $\theta, \omega$  from  $\mathbf{p}_{1n}$  using (5), (6)
4   for  $i = 2$  to  $n - 1$  do
5     if  $\tau_{1i}$  exists such that  $\mathbf{D}'_k$  lies in the
       neighborhood  $(\epsilon_p, \epsilon_\phi)$  of  $\mathbf{D}_k$  then
6       continue
7     else
8       return false
9   return true

```

Algorithm 2: Check if motion is pure rotation or general screw

```

1 def checkIfGeneralScrew( $\mathcal{D}, \epsilon_p, \epsilon_\phi$ ):
2   Determine  $\mathbf{Q}_{1n}$  and  $\mathbf{p}_{1n}$  from  $\mathbf{D}_{1n} = \mathbf{D}_n \otimes \mathbf{D}_1^*$ 
3   Get  $\theta, \omega$  from  $\mathbf{Q}_{1n}$ , and  $h, \mathbf{m}$  from  $\mathbf{p}_{1n}$  using (8)
      and (7)
4   for  $i = 2$  to  $n - 1$  do
5     if  $\tau_{1i}$  exists such that  $\mathbf{D}'_k$  lies in the
       neighborhood  $(\epsilon_p, \epsilon_\phi)$  of  $\mathbf{D}_k$  then
6       continue
7     else
8       return false
9   return true

```

Algorithm 3: Determination of Screw Parameters

```

1 def getScrewParameters( $\mathcal{D}, \epsilon_p, \epsilon_\phi$ ):
2    $\mathbf{D}_{1n} = \mathbf{D}_n \otimes \mathbf{D}_1^*$ 
3   if checkIfPrismatic( $\mathcal{D}, \epsilon_p, \epsilon_\phi$ ) is true then
4     Compute  $\omega, \theta$  from  $\mathbf{D}_{1n}$  using (5),
       $h = \infty, \mathbf{m} = \mathbf{0}$ 
5     return  $\omega, \mathbf{m}, \theta, h$ 
6   else if checkIfGeneralScrew( $\mathcal{D}, \epsilon_p, \epsilon_\phi$ ) is
      true then
7     Compute  $\omega, \theta, h, \mathbf{m}$  from  $\mathbf{D}_{1n}$  using (2), (8),
      (3), (7)
8     return  $\omega, \mathbf{m}, \theta, h$ 
9   else
10    return  $\mathcal{D}$  is not generated by a single screw

```

Algorithm 2 is similar to Algorithm 1 but gives the procedure to check if the given motion \mathcal{D} belongs to the category of general screw or pure rotational motion ($h \neq \infty$).

Algorithm 3 gives the procedure to compute the constant screw parameters of the given motion \mathcal{D} . It takes as input the sequence of poses \mathcal{D} and the parameters $\epsilon_p, \epsilon_\phi$ to define the size of the neighborhood, and returns the constant screw parameters if the motion \mathcal{D} was generated by a constant

screw motion. It first checks if the given motion is pure translation and if it is true then computes the screw parameters as mentioned in line 4. If the motion is not pure translation, but a general screw or pure rotation, then it computes the screw parameters as mentioned in line 7. If the previous two conditions are not satisfied, then the given motion \mathcal{D} is not generated by a constant screw motion.

It is important to note that due to the presence of noise, motion that results from prismatic motion might be fit to a general screw with $h \neq \infty$ depending on choice of the parameters ε_p and ε_ϕ . Also, in section V-B, we will be showing how we can extend this check to segment any given sequence of $SE(3)$ poses into a sequence of constant screws.

B. Segmentation of a Sequence of Screws

If the sequence \mathcal{D} was generated by a sequence of constant screw motions, then we can represent the motion as a sequence of screw displacements $\delta_1, \delta_2, \dots, \delta_u$ applied to the initial pose \mathbf{D}_1 where $1 \leq u < n$, or as a sequence of rigid body poses $\{\mathbf{E}_1, \mathbf{E}_2, \dots, \mathbf{E}_u\}$ where $\mathbf{E}_1 = \delta_1 \otimes \mathbf{D}_1$ and $\mathbf{E}_i = \delta_i \otimes \mathbf{E}_{i-1}$ for $i = 2, \dots, u$. Here, \mathbf{E}_i represents the end pose of each constant screw segment in sequence and u represents the number of constant screws present in the motion \mathcal{D} . If $u = 1$, then this reduces to the case of single screw motion discussed previously in Section V-A. While in some cases the representation based on screw parameters is useful, in other cases the representation based on $SE(3)$ poses is useful and we will be going back and forth between these representations in this paper.

As stated before, according to Chasles Theorem, any rigid body displacement between two given poses can be expressed as a constant screw motion. So given two poses \mathbf{D}_1 and \mathbf{D}_2 , the rigid body displacement can be realised by the screw motion $\delta = \mathbf{D}_2 \otimes \mathbf{D}_1^*$ with screw parameters $(\omega, \mathbf{m}, h, \theta)$ and any pose \mathbf{D}_τ on the screw motion between \mathbf{D}_1 and \mathbf{D}_2 can be computed using the parameters $(\omega, \mathbf{m}, h, \tau\theta)$, $0 \leq \tau \leq 1$.

Ideally, if the sequence $\{\mathbf{D}_i, \mathbf{D}_{i+1}, \dots, \mathbf{D}_{j-1}, \mathbf{D}_j\}$ has been generated by a constant screw, then $\forall i < k \leq j \exists \theta_k$ such that, $\mathbf{D}_k = \mathbf{D}_{ik} \otimes \mathbf{D}_i$, where $\mathbf{D}_{ik} = \mathbf{Q}_{ik} + \frac{\varepsilon}{2} \mathbf{p}_{ik} \otimes \mathbf{Q}_{ik}$, with screw parameters $(\omega_{ij}, \mathbf{m}_{ij}, h_{ij}, \theta_{ik})$. But, due to the presence of noise, \mathbf{D}_k does not lie on the ideal screw motion from \mathbf{D}_i to \mathbf{D}_j . However, as discussed before, we can determine a θ_{ik} which gives us \mathbf{D}'_k that lies within a neighbourhood $(\varepsilon_p, \varepsilon_\phi)$ of the pose \mathbf{D}_k . If no such θ_k exists then \mathbf{D}_k does not lie on the screw motion from \mathbf{D}_i to \mathbf{D}_j and this means that the sequence $\{\mathbf{D}_i, \mathbf{D}_{i+1}, \dots, \mathbf{D}_{j-1}, \mathbf{D}_j\}$ is not generated by a constant screw.

This is the same check we discussed previously in Section V-A and using this procedure as a test to determine whether the given sequence of $SE(3)$ poses is generated by a constant screw or not, we determine the indices i, j for all the u constant screw segments present in the sequence \mathcal{D} .

Algorithm 4 uses Algorithm 3 to determine the start pose \mathbf{D}_i and end pose \mathbf{D}_j of each screw segment in the given $SE(3)$ pose sequence such that all the intermediate poses $\mathbf{D}_{i+1}, \dots, \mathbf{D}_{j-1}$ can be fit within a given tolerance $(\varepsilon_p, \varepsilon_\phi)$ to the ideal screw from \mathbf{D}_i to \mathbf{D}_j .

Algorithm 4: Segment given motion into a sequence of constant screws

```

1 def getScrewSegments( $\mathcal{D}, \varepsilon_p, \varepsilon_\phi$ ) :
2     Set  $u = 1, i = 1, \mathbf{E}_u = \mathbf{D}_n$ 
3     while  $i <= n$  do
4         for  $j = i + 1$  to  $n$  do
5              $\mathcal{D}' = \{\mathbf{D}_i, \dots, \mathbf{D}_j\}$ 
6             if getScrewParameters( $\mathcal{D}', \varepsilon_p, \varepsilon_\phi$ )
7                 returns  $\omega, \mathbf{m}, \theta, h$  then
8                     continue
9                  $\mathbf{E}_u = \mathbf{D}_{j-1}$ 
10                 $u = u + 1$ 
11                 $i = j$ 
12                break
13
14 return  $\{\mathbf{E}_1, \mathbf{E}_2, \dots, \mathbf{E}_u\}$ 

```

The output of Algorithm 4 is the segmentation of the motion of the end effector in the task space as a sequence of constant screws. This sequence of constant screws describe the task constraints in a coordinate invariant manner, i.e., it does not depend on the choice of the end effector coordinate frame. By extracting the task constraints which are enforced either due to the presence of joints or due to the inherent nature of the task, we are able to generalize a single demonstration to different task instances using the planning method described in Section VI.

VI. MOTION GENERATION FROM SEGMENTED DEMONSTRATION

In this section, we will describe our method of motion generation based on the description of a demonstrated motion as a sequence of screw segments (along with the poses of the objects, if any). As stated before, we consider manipulation tasks belonging to two different classes. First, we consider manipulation of articulated objects, which is usually accomplished by a single constant screw motion. Second, we consider complex manipulation tasks that can be executed by a sequence of constant screw motions.

A. Manipulation of Articulated Objects

Problem Statement: Given a single demonstration $\mathcal{D} = \{\mathbf{D}_1, \mathbf{D}_2, \dots, \mathbf{D}_n\}$ for manipulating articulated objects, determine the motion plan required to manipulate the articulated object for a new initial pose \mathbf{D}'_1 of the end-effector and magnitude of motion θ'

Articulated objects are constrained in their motion based on the type of joint (revolute/prismatic) present. Given the screw parameters of the joints, we can compute the motion of the end-effector required to manipulate the objects. We determine these parameters $(\omega, \mathbf{m}, h, \theta)$ from $\delta = \mathbf{D}_n \otimes \mathbf{D}'_1$.

Here θ is just the magnitude of the screw motion and can be changed depending on the direction or the magnitude by

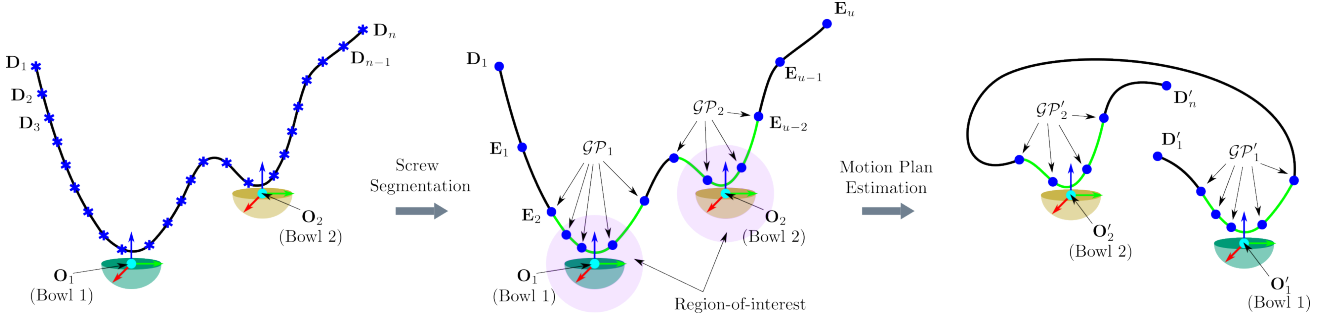


Fig. 4: SCHEMATIC SKETCH FOR MOTION ESTIMATION OF COMPLEX TASK: Overview of motion estimation for a scoop and pour task. The task involves scooping contents from Bowl 1 with a spoon and pouring it into Bowl 2. The $SE(3)$ poses are represented as points to reduce clutter; **Left** - The provided demonstration \mathcal{D} consisting of a sequence of $SE(3)$ poses along with pose of the objects O_1 (Bowl 1) and O_2 (Bowl 2); **Center** - Segmenting the provided demonstration \mathcal{D} into a sequence of constant screws $\{D_1, E_1, \dots, E_u\}$ and determining the **Key Segments** (Coloured Green) associated with each object. The task-relevant constraints \mathcal{GP}_1 (Bowl 1), \mathcal{GP}_2 (Bowl 2) are identified from the Key Segments; **Right** - Computing the motion plan for new initial pose D'_1 , final pose D'_2 and object poses O'_1 (Bowl 1) and O'_2 (Bowl 2) by determining the **Guiding Poses** \mathcal{GP}' utilizing the task-relevant constraints (Coloured Green) obtained from the previous step

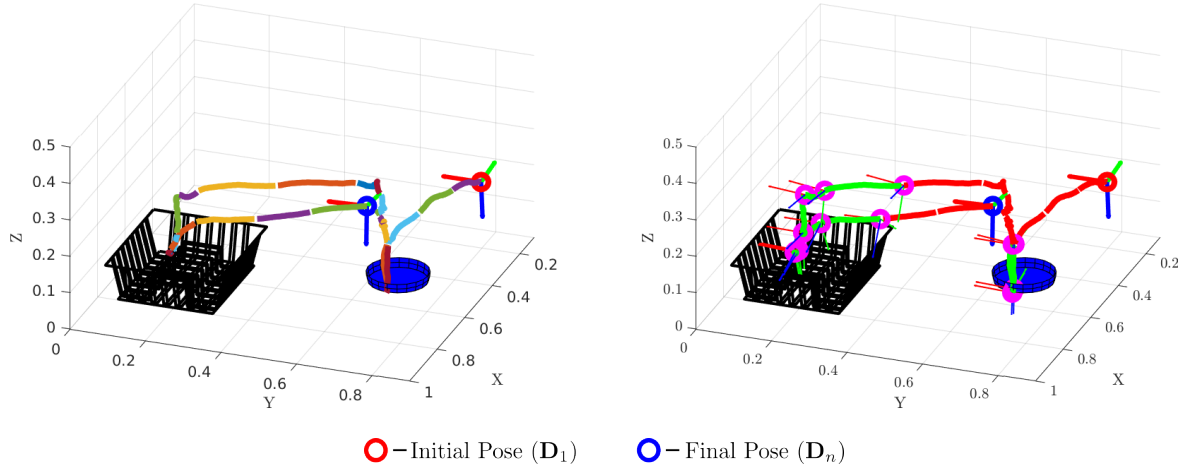


Fig. 5: RECORDED DEMONSTRATION FROM ARRANGING DISHES TASK EXPERIMENT: Recorded end-effector trajectory as a sequence of $SE(3)$ poses from an actual demonstration. Majority of the recorded $SE(3)$ poses are hidden to reduce clutter; **Left** - Segmentation of the provided demonstration \mathcal{D} into a sequence of constant screws. The constant screw segments are differentiated using different colours; **Right** - The **Key Segments** are coloured green and the \mathcal{GP}_i poses are represented using Magenta coloured markers

which we want to move the object. For example, we can vary the angle by which we open/close the door about its hinge using θ . Once we have estimated the screw parameters, given a new initial pose D'_1 of the end-effector and magnitude of motion θ' , we can use the screw parameters to compute the screw displacement $\delta' = (\cos \frac{\theta' + \epsilon h \theta'}{2}, (\omega + \epsilon m) \sin \frac{\theta' + \epsilon h \theta'}{2})$ and the new final configuration $D'_n = \delta' \otimes D'_1$. Once we have determined the goal pose D'_n , we can compute the motion plan from D'_1 to D'_n which is required to manipulate the articulated object using the ScLERP motion planner [21] so that the motion satisfies the screw constraint. Note that our approach does not need *a priori* information about the articulation model to estimate the joint constraints. Further, the fact that ScLERP will generate poses of the end-effector that satisfies the constraint imposed by the joint without explicitly considering it is proven in [21].

B. Complex Manipulation Tasks

Problem Statement: Given a single demonstration of a task $\mathcal{D} = \{D_1, D_2, \dots, D_n\}$ and the poses $\{O_1, O_2, \dots, O_v\}$ of the v task-relevant objects during the demonstration, compute the motion plan required to perform the task for new poses for the initial pose, D'_1 and final pose, D'_n and the task-relevant objects $\{O'_1, O'_2, \dots, O'_v\}$

For complex manipulation tasks we segment the provided demonstration into a sequence of constant screws which can then be used to determine the task constraints and generate the motion plan for a new task instance.

Determination of Task Relevant Constraints: The task-relevant constraints that are implicitly present in the provided demonstration are approximated as a sequence of constant screws. Based on a heuristic that the task-relevant constraints occur in a region-of-interest surrounding the task-relevant objects, we define the task-relevant constraints as *the sequence*

of screw segments obtained from the provided demonstration such that they lie inside the region-of-interest surrounding the task-related objects and expressed with respect to the local frame of reference of the associated task-related object. Each task-relevant object has its own region-of-interest and a sequence of screws associated with it. Let us refer to the screw segments that lie inside a region-of-interest as **key segments**. Here, we define the region-of-interest of a task-related object to be a spherical volume or a cuboid centered at the object frame with dimensions that is set based on the type of the object. However it can also be chosen to be any other shape that captures the motion that is associated with the task-relevant objects.

We segment the provided demonstration \mathcal{D} into a sequence of u constant screws $\{\mathbf{E}_1, \mathbf{E}_2, \dots, \mathbf{E}_u\}$, $u \leq (n - 1)$ (We will be using $SE(3)$ poses to represent screw segments). Then, we construct the regions-of-interest for all the v task-relevant objects at $\{\mathbf{O}_1, \mathbf{O}_2, \dots, \mathbf{O}_v\}$ and determine the key segments associated with each object (Figure 5).

The key-segments associated with each task related object i are determined as $\{\mathbf{G}_{i,1}, \mathbf{G}_{i,2}, \dots, \mathbf{G}_{i,m_i}\}$, where m_i is the number of key-segments associated with the object.

The task-relevant constraints for object i expressed in its local frame of reference are then computed as,

$$\mathcal{GP}_i = \{\mathbf{O}_i^* \otimes \mathbf{G}_{i,1}, \mathbf{O}_i^* \otimes \mathbf{G}_{i,2}, \dots, \mathbf{O}_i^* \otimes \mathbf{G}_{i,m_i}\} \quad (9)$$

Generation of Motion Plan for a new task instance: Given the new poses of the task related objects, $\{\mathbf{O}'_1, \mathbf{O}'_2, \dots, \mathbf{O}'_v\}$, we can re-compute the task-relevant constraints with respect to the new pose of the object.

For the new pose \mathbf{O}'_i of each object i , the task-relevant constraints can be computed from (9) as

$$\mathcal{GP}'_i = \{\mathbf{O}'_i \otimes \mathbf{O}_i^* \otimes \mathbf{G}_{i,1}, \dots, \mathbf{O}'_i \otimes \mathbf{O}_i^* \otimes \mathbf{G}_{i,m_i}\} \quad (10)$$

Once the task-relevant constraints for the new task instance have been computed, we construct the sequence of constant screws that the end-effector should follow to successfully execute the task. We define this sequence as the **Guiding Poses**. The guiding poses can be constructed as,

$$\mathcal{GP}' = \{\mathbf{D}'_1, \mathcal{GP}'_1, \mathcal{GP}'_2, \dots, \mathcal{GP}'_v, \mathbf{D}'_n\} \quad (11)$$

The guiding poses \mathcal{GP}' define the motion plan for the given new instance of the task. Using the ScLERP Motion Planner [21] to move to each of the poses in \mathcal{GP}' ensures that the task-relevant constraints are satisfied while the motion is being executed.

VII. EXPERIMENTAL RESULTS

In this section we provide experimental results for four manipulation tasks that can be classified into two categories: (a) manipulation of articulated objects, and (b) complex manipulation tasks. For category (a), we consider two tasks: (1) manipulation of an object constrained by a revolute joint (2) manipulation of an object constrained by a prismatic joint, and for category (b), we consider two tasks: (3) scooping and

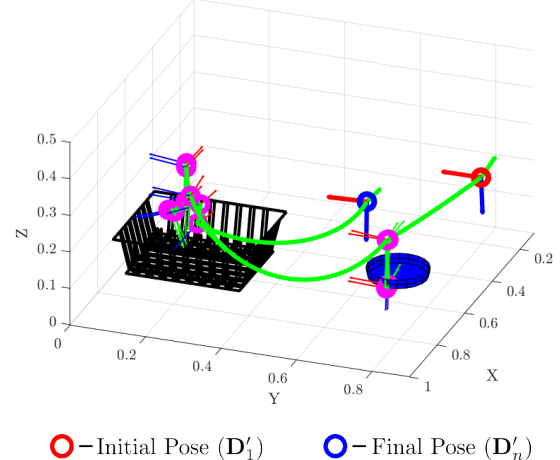


Fig. 6: MOTION PLAN FOR A NEW TASK INSTANCE OF THE ARRANGING DISHES TASK: The motion plan is computed by determining the **Guiding Poses**, \mathcal{GP}' (Magenta coloured markers) as detailed in Section VI-B for the new initial pose, final pose and object poses. The final motion (Green coloured trajectory) is obtained by interpolating using ScLERP between consecutive guiding poses

pouring (4) arranging dishes in a rack. We conducted a total of 118 experimental trials over the four manipulation tasks.

The experiments are performed using the Baxter robot from Rethink Robotics [19]. A demonstration is provided using a kinesthetic interface. During a demonstration, the joint angles are recorded, and by using the forward kinematics map of the robot, we obtain the sequence of poses in $SE(3)$, which is segmented to compute the sequence of constant screw motions that capture the task constraints.

A. Manipulation of Articulated Objects

For each task, we test our algorithm on 3 different demonstrations. For each demonstration, the gripper held the object in a different place with a different pose. For each demonstration, we perform 13 experimental trials with the extracted screw, where the gripper pose varied across the different trials and were different from that in the demonstration. Thus, we conducted a total of 78 experimental trials (39 for each task). The purpose of varying the gripper poses is to show that, practically, the coordinate invariance implies that irrespective of how we hold the object, we can use the extracted screw from just a single demonstration to manipulate the object.

Recall that we had two parameters in our segmentation algorithm, namely, ε_p and ε_ϕ . Across all our experiments, we set the values of the parameters as $\varepsilon_p = 1$ cm and $\varepsilon_\phi = 0.1$.

1) **Object constrained by a Revolute Joint:** The object used for this task is a wooden block constrained to rotate about a revolute joint. Figure 3 shows the object and snapshots of one demonstration. For this experiment, although the demonstrations were for opening the wooden block, the robot was made to perform the task of both opening and closing it. The pose of the gripper was changed between each trial by moving the gripper along the length of the handle and also changing the

orientation of the gripper. This task was split into two test cases, namely, (a) opening by an angle of 45° from its closed position, and (b) closing by an angle of 45° from its open position.

For each of the 3 demonstrations, the task of opening was performed 8 times and the task of closing was performed 5 times. Figure 8 shows the change of the gripper poses for different trials. For all the trials, the robot was able to successfully open/close the wooden block by the given magnitude of 45° about the revolute joint. Even though all the provided demonstrations were of opening the block, by using the extracted screw parameters with only a change in the sign of the magnitude of the screw, we were also able to perform the task of closing the block.

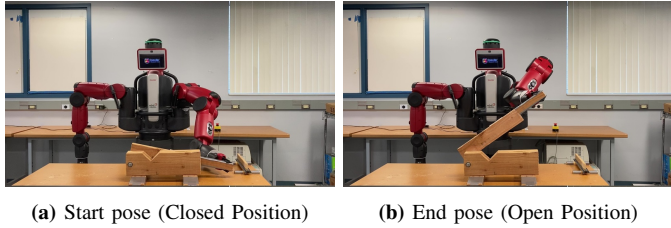


Fig. 7: REVOLUTE JOINT: Trial 7 using Demonstration 3

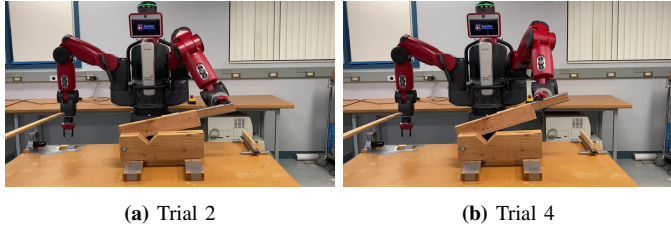


Fig. 8: GRASPING POSE CHANGES - REVOLUTE JOINT EXPERIMENT: Changes in position and orientation of the end-effector along the handle of the wooden block between different trials using Demonstration 3

Demo	ω	θ (deg)	h
1	$[0.9992 \ 0.0264 \ -0.0293]^T$	41.01	0.0202
2	$[0.9997 \ 0.0188 \ -0.0152]^T$	39.97	0.0117
3	$[0.9881 \ 0.1439 \ 0.0551]^T$	38.36	0.0053

TABLE I: Revolute Joint - Screw Parameters computed from recorded demonstrations

Table I shows some relevant screw parameters for the three demonstrations of moving the wooden block constrained by a revolute joint. The second column shows the screw axis, which in this case is the same as the axis of the revolute joint. Note that the computation has been done using the poses of the gripper for which both the position and the orientation changes. However, the pitch (shown in the last column) is almost 0, which shows that the motion is generated by a pure rotation. The slight deviation from 0 in the estimated pitch is due to the presence of noise in the joint encoders and clearance

in the revolute joint. Furthermore, the estimated axis of the revolute joint is almost identical (within the noise range).

2) Object constrained by a Prismatic Joint: The object used for this task is a wooden block constrained to translate along a prismatic joint axis (see Fig. 3). This task was also categorized into two cases, namely, (a) opening from the closed position by a distance of 30 cm, and (b) closing from the open position by a distance of 30 cm. Among the 3 demonstrations, the first and the second was that of opening the block from the closed position while the third demonstration was that of closing the block from the open position. For each demonstration, opening was performed 8 times and closing the block was performed 5 times with a random grasping pose for each trial (See Figure 10).

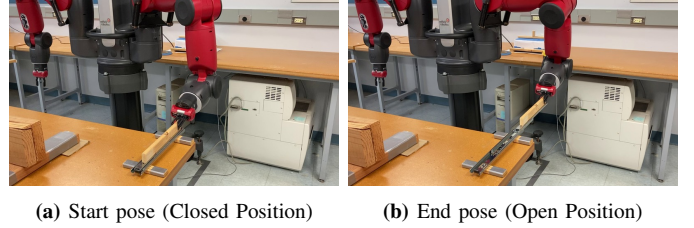


Fig. 9: PRISMATIC JOINT: Trial 2 using Demonstration 3



Fig. 10: GRASPING POSE CHANGES - PRISMATIC JOINT EXPERIMENT: Changes in position and orientation of the end-effector between different trials using Demonstration 3

All of the experimental trials were successful and as before changing the sign of the screw magnitude allowed us to accomplish both opening and closing tasks even though the demonstration may be of the opposite type. Here again, the importance of using the screw geometry of motion is highlighted by the fact that all the 39 trials were performed successfully irrespective of the pose at which the end effector grasped the object (See Figure 10).

Demo	ω	θ (m)
1	$[-0.9997 \ -0.0169 \ 0.0199]^T$	0.3270
2	$[-0.9989 \ -0.0147 \ 0.0452]^T$	0.3207
3	$[0.9995 \ 0.0257 \ -0.0184]^T$	0.3209

TABLE II: Prismatic Joint - Screw Parameters computed from recorded demonstrations

Table II shows some of the screw parameters for the prismatic joint obtained from the three demonstrations. Here, the estimated screw axis, ω is same as the axis of the prismatic

joint. The estimated joint axis only vary slightly due to the presence of noise in the joint encoders and the clearance in the joint. Note that the estimated joint axis for the third demonstration is in the opposite direction compared to the first two demonstrations. This is because, in the third demonstration, we were closing (or pushing) the block, whereas we were opening (or pulling) the block in the first two demonstrations.

B. Complex Manipulation Tasks

For complex manipulation tasks, along with the kinesthetic demonstration, we also record the poses of the task related objects. We segment the end-effector path into a sequence of constant screws and extract the key segments. During task execution, we vary the pose of the task-related objects. Given the new poses of the objects, we compute the guiding poses and use those to determine the new motion plan. The values of the screw segmentation parameters for complex manipulation tasks was set as $\varepsilon_p = 1$ cm and $\varepsilon_\phi = 0.15$.

1) **Scooping and Pouring:** In this task the robot scoops rice from one bowl using a spoon which the robot is already grasping and pours it into another bowl which is placed at a different position (see Figure 11). The radius of the region of interest used for obtaining the key segments is 20 cm.

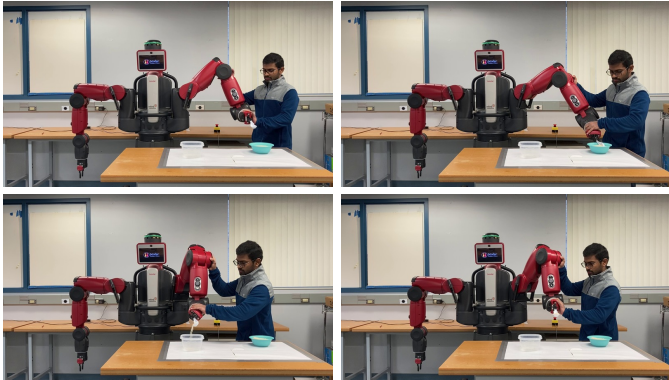


Fig. 11: SCOOP AND POUR: Demonstration 1
(Clockwise from top left)

Two demonstrations were given with different poses of the objects. For each demonstration we extracted the task-relevant screws, and used it to compute motion plans for eight experimental trials. Thus a total of 16 experimental trials were performed for this task. Each trial was conducted by varying pose of one or both the bowls. In particular, the heights of the bowls were also changed among some trials, so that merely mimicking the demonstrated path would result in a collision. During each trial, it was ensured that the level of rice in the bowl was the same as in the demonstration. Due to the lack of perception, our framework cannot account for the level of rice in the bowl. All of the trials resulted in successful scooping and transfer of rice from one bowl to another.

2) **Arranging Dishes:** In this task we pick a plate placed on the table and insert it into one of the slots of a dish rack that is placed on the table. This exemplar task was chosen because it consists of a challenging collision avoidance problem when

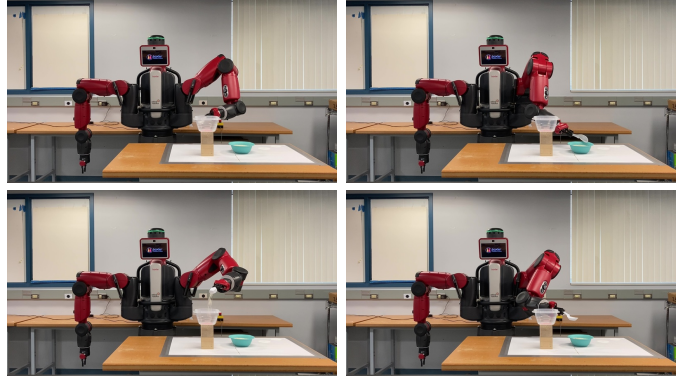


Fig. 12: SCOOP AND POUR: Trial 8 using Demonstration 1
(Clockwise from top left)

the dish has to be placed in the dish rack. The geometry of the dishes and the slots of the dish rack are such that putting in the dishes top down vertically would result in the dish getting jammed and not reaching the bottom of the rack. The dish has to be put in at an angle and moved in a way that is hard to describe in words or write equations for, but easier for a human to demonstrate. There were 3 different demonstrations provided and for each demonstration, we performed 8 experimental trials. Thus, a total of 24 experimental trials were performed. To extract the key segments the region of interest were chosen to be a sphere of radius 15 cm for the dish and a cube of side 45 cm for the dish rack. The key segments were extracted from the demonstration and the guiding poses were determined with the knowledge of the new pose of the task related objects (plate and dish rack). The motion plan was determined using the guiding poses. Also, the grasping information, i.e., where the gripper should be closed relative to the pose of the object is determined from the demonstration and is used to grasp the object during execution.

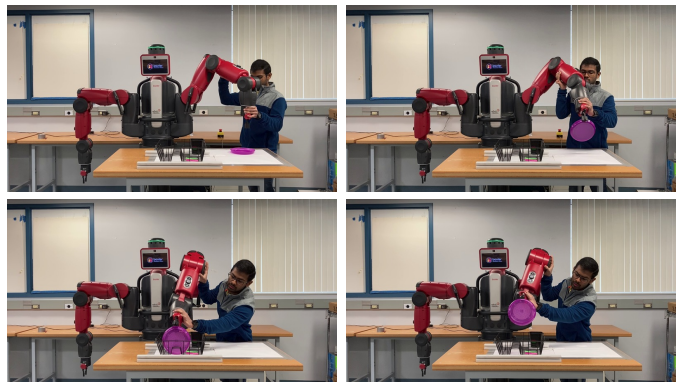


Fig. 13: ARRANGING DISHES: Demonstration 3
(Clockwise from top left)

For this task, a trial is considered to be a success if the robot can pick up the dish from the table and insert it into the correct slot in the dish rack. If not, the trial is considered to be a failure. Table III shows the results of the eight trials for all the three demonstrations. Among the different trials, the pose

Demonstration	Number of Trials	Successful Trials	Failed Trials
Demonstration 1	8	7	1
Demonstration 2	8	8	0
Demonstration 3	8	5	3

TABLE III: Arranging Dishes - Trials

of the dish, the dish rack, as well as the slot in which the dish is being inserted was varied. All the failures are related to the joint accuracy limits of Baxter. Due to these inaccuracies, the plate was either placed in the neighbouring slot instead of the intended slot or hit the raised edges of the rack and got stuck.

We also performed one trial of inserting multiple dishes into the dish rack using the example of insertion of a single dish. Figure 15 shows snapshots from the experimental trial. This trial was meant as a proof-of-concept demonstration and we plan to perform more extensive experimental evaluation of this scenario in future work.

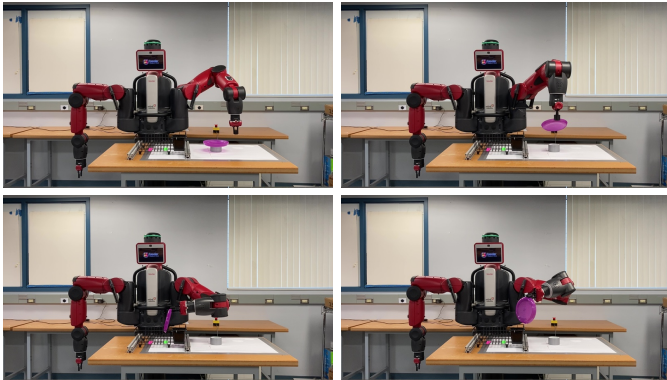


Fig. 14: ARRANGING DISHES: Trial 12 using Demonstration 3 (Clockwise from top left)

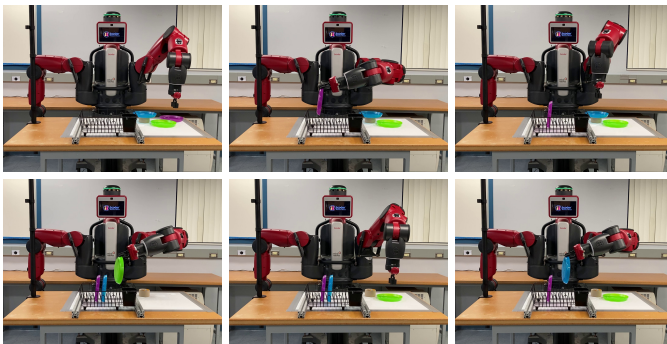


Fig. 15: ARRANGING DISHES: Arranging multiple dishes using a single demonstration (Clockwise from top left)

C. Discussion

Since we are trying to extract the implicit constraints embedded in a motion through a kinesthetic guidance demonstration, there is an underlying assumption that the demonstrator is benevolent or trying to help the robot. As discussed above, although there is no strict requirement about how an object

should be held during the task, it is assumed that the object is held in such a way that the required motion can be performed and there is no slippage between the object and the robot gripper during the demonstration.

In principle, the extracted screw segments can be used to transfer the constraints to any task instance and provide us a feasible motion plan in the task space. However, within the ScLERP based motion planner, we are using the Jacobian pseudoinverse to compute the joint space motion from the task space motion. Thus, our motion planner is susceptible to the limitations of the Jacobian pseudoinverse based planning schemes, like hitting joint limits, especially if the robot is working near the boundary of its workspace. Although there are solutions for these problems that utilize the nullspace of the Jacobian to move away from the joint limits [13], these solutions do not guarantee that the planner will not get stuck. For mobile manipulation, one possible solution is to position the base in such a way that the task region is not too close to the boundary of the workspace (which we have done in our experiments). Another possible solution is to evaluate its current demonstration for different task instances in simulation and then actively seek demonstration from a human in regions that it gets stuck. We are currently exploring this approach.

VIII. CONCLUSION AND FUTURE WORK

The expression of task constraints as a sequence of constant screws allows us to exploit the structure of motion present in complex manipulation tasks. While expressing these task constraints in the joint space is a hard problem, expressing them as a sequence of constant screws allows us to represent them in a coordinate-invariant manner. In this paper, we have presented an approach to use a single kinesthetic demonstration for extracting the task constraints as a sequence of constant screws. Using this approach, we also show how these computed constant screws can be used to plan motion for a new task instance. For evaluating this approach, we conducted multiple experiments to manipulate articulated objects and perform complex manipulation tasks from a single demonstration. For articulated objects, we were able to generalize to variations in position and orientation of where the robot grasps the object for manipulation. For complex manipulation tasks, we were able to generalize to variations in position and orientation of the task related objects.

The expression of task constraints as a sequence of constant screws in the task-space would potentially allow us to provide demonstrations on one robot and execute the task on another robot with completely different hardware architectures. The proposed method does not take collision avoidance into consideration. Either, there might be an obstacle on the interpolated path between the guiding poses that the end-effector needs to follow, or there might be an obstacle that might come in contact with one of the robot links even when the end-effector does not collide with objects when following the required interpolated path. While the latter case can be overcome by integrating obstacle avoidance in the ScLERP based motion planner as proposed in [23], the former case

requires modifying the task constraints. In future work we plan on incorporating collision avoidance with the current approach. Also, the heuristic used to determine the guiding poses associated with each object can be improved.

REFERENCES

- [1] B. Abbatematteo, S. Tellex, and G. Konidaris. Learning to generalize kinematic models to novel objects. In L. P. Kaelbling, D. Kragic, and K. Sugiura, editors, *Proceedings of the Conference on Robot Learning*, volume 100 of *Proceedings of Machine Learning Research*, pages 1289–1299. PMLR, 30 Oct–01 Nov 2020.
- [2] A. G. Billard, S. Calinon, and R. Dillmann. *Learning from Humans*, pages 1995–2014. Springer International Publishing, Cham, 2016.
- [3] S. Calinon, F. D’halluin, E. L. Sausser, D. G. Caldwell, and A. G. Billard. Learning and reproduction of gestures by imitation. *IEEE Robotics & Automation Magazine*, 17(2):44–54, 2010.
- [4] S. Calinon, F. Guenter, and A. Billard. On learning, representing, and generalizing a task in a humanoid robot. *IEEE Transactions on Systems, Man, and Cybernetics, Part B (Cybernetics)*, 37(2):286–298, 2007.
- [5] S. Calinon, A. Pistillo, and D. G. Caldwell. Encoding the time and space constraints of a task in explicit-duration hidden markov model. In *2011 IEEE/RSJ International Conference on Intelligent Robots and Systems*, pages 3413–3418, 2011.
- [6] J. De Schutter. Invariant Description of Rigid Body Motion Trajectories. *Journal of Mechanisms and Robotics*, 2(1), 11 2009. 011004.
- [7] M. Hersch, F. Guenter, S. Calinon, and A. Billard. Dynamical system modulation for robot learning via kinesthetic demonstrations. *IEEE Transactions on Robotics*, 24(6):1463–1467, Dec 2008.
- [8] D. Q. Huynh. Metrics for 3d rotations: Comparison and analysis. *Journal of Mathematical Imaging and Vision*, 35(2):155–164, 2009.
- [9] A. J. Ijspeert, J. Nakanishi, H. Hoffmann, P. Pastor, and S. Schaal. Dynamical movement primitives: Learning attractor models for motor behaviors. *Neural Comput.*, 25(2):328–373, Feb. 2013.
- [10] A. Jain, R. Lioutikov, C. Chuck, and S. Niekum. Screwnet: Category-independent articulation model estimation from depth images using screw theory. In *arXiv preprint*, 2020.
- [11] R. Laha, A. Rao, L. F. C. Figueiredo, Q. Chang, S. Hadadin, and N. Chakraborty. Point-to-Point Path Planning Based on User Guidance and Screw Linear Interpolation. volume Volume 8B: 45th Mechanisms and Robotics Conference (MR) of *International Design Engineering Technical Conferences and Computers and Information in Engineering Conference*, 08 2021. V08BT08A010.
- [12] S. H. Lee, I. H. Suh, S. Calinon, and R. Johansson. Autonomous framework for segmenting robot trajectories of manipulation task. *Autonomous Robots*, 38(2):107–141, Feb 2015.
- [13] A. Liégeois. Automatic supervisory control of the configuration and behavior of multibody mechanisms. *IEEE Transactions on Systems, Man, and Cybernetics*, 7(12):868–871, 1977.
- [14] F. Meier, E. Theodorou, F. Stulp, and S. Schaal. Movement segmentation using a primitive library. In *2011 IEEE/RSJ International Conference on Intelligent Robots and Systems*, pages 3407–3412, 2011.
- [15] P. Mike, V. Hwang, S. Chitta, and M. Likhachev. Learning to plan for constrained manipulation from demonstrations. In *Proceedings of Robotics: Science and Systems*, Berlin, Germany, June 2013.
- [16] H. B. Mohammadi, S. Hauberg, G. Arvanitidis, G. Neumann, and L. D. Rozo. Learning riemannian manifolds for geodesic motion skills. In *Robotics: Science and Systems*, 2021.
- [17] R. M. Murray, Z. Li, and S. S. Sastry. *A mathematical introduction to robotic manipulation*. CRC press, 1994.
- [18] P. Pastor, H. Hoffmann, T. Asfour, and S. Schaal. Learning and generalization of motor skills by learning from demonstration. In *2009 IEEE International Conference on Robotics and Automation*, pages 763–768, May 2009.
- [19] R. Robotics. Baxter hardware specifications. https://sdk.rethinkrobotics.com/wiki/Hardware_Specifications.
- [20] T. Rühr, J. Sturm, D. Pangercic, M. Beetz, and D. Cremer. A generalized framework for opening doors and drawers in kitchen environments. In *2012 IEEE International Conference on Robotics and Automation*, pages 3852–3858, May 2012.
- [21] A. Sarker, A. Sinha, and N. Chakraborty. On screw linear interpolation for point-to-point path planning. In *2020 IEEE/RSJ International Conference on Intelligent Robots and Systems (IROS)*, pages 9480–9487, 2020.
- [22] M. Saveriano, F. Franzel, and D. Lee. Merging position and orientation motion primitives. In *2019 International Conference on Robotics and Automation (ICRA)*, pages 7041–7047, May 2019.
- [23] A. Sinha, A. Sarker, and N. Chakraborty. Task Space Planning With Complementarity Constraint-Based Obstacle Avoidance. volume Volume 8B: 45th Mechanisms and Robotics Conference (MR) of *International Design Engineering Technical Conferences and Computers and Information in Engineering Conference*, 08 2021. V08BT08A012.
- [24] J. Sturm, V. Pradeep, C. Stachniss, C. Plagemann, K. Konolige, and W. Burgard. Learning kinematic models for articulated objects. In *Proceedings of the 21st International Joint Conference on Artificial Intelligence, IJCAI’09*, page 1851–1856, San Francisco, CA, USA, 2009. Morgan Kaufmann Publishers Inc.
- [25] J. Sturm, C. Stachniss, and W. Burgard. A probabilistic framework for learning kinematic models of articulated objects. *J. Artif. Int. Res.*, 41(2):477–526, may 2011.
- [26] M. Vochten, T. De Laet, and J. De Schutter. Generalizing

demonstrated motion trajectories using coordinate-free shape descriptors. *Robotics and Autonomous Systems*, 122:103291, 2019.